

## **Supplemental Material**

# **Physiologically Based Pharmacokinetic (PBPK) Modeling of Interstrain Variability in Trichloroethylene Metabolism in the Mouse**

Weihsueh A. Chiu, Jerry L. Campbell Jr., Harvey J. Clewell 3<sup>rd</sup>, Yi-Hui Zhou, Fred A. Wright,  
Kathryn Z. Guyton, and Ivan Rusyn

<b>Table of Contents</b>	<b>Page</b>
<b>Figure S1.</b> Histograms of the transformed values and quantile-quantile plots for TCE metabolites TCA, DCA, DCVG and DCVC.	3
<b>Figure S2.</b> Schematic of the modified Hack et al. (2006) model.	4
<b>Figure S3.</b> Monte Carlo simulation (100 iterations) of the multistain mouse time-course data with the parameter distributions for metabolism and clearance of metabolites estimated to fit the range of measured values.	5
<b>Figure S4.</b> Comparison of data and PBPK model predictions for TCA in mouse inbred strains.	6
<b>Figure S5.</b> Comparison of data and PBPK model predictions for DCA in mouse inbred strains.	8
<b>Figure S6.</b> Comparison of data and PBPK model predictions for DCVG in mouse inbred strains.	10
<b>Figure S7.</b> Comparison of data and PBPK model predictions for DCVC in mouse inbred strains.	12
<b>Table S1.</b> TCE metabolite data for individual mice (rows) of AKR/J and WSB/EiJ strains.	14
<b>Table S2.</b> Parameter distributions estimated with Monte Carlo analysis of the multistain mouse data.	15
<b>Table S3.</b> PBPK model parameters, baseline values, and scaling relationships.	16

<b>Table S4.</b> Uncertainty distributions for the population mean and variance of the PBPK model parameters.	<b>25</b>
<b>Table S5.</b> Interstrain variability parameters.	<b>29</b>
<b>Table S6.</b> Comparison of prior and posterior distributions for scaling parameters.	<b>30</b>
<b>Methods</b>	<b>32</b>
Details of the Bayesian PBPK modeling of TCE and its metabolites	32
PBPK model structure and equations	32
TCE submodel	33
Gas exchange, respiratory metabolism, arterial blood concentration, and closed-chamber concentrations	33
Oral absorption to gut compartment	35
Nonmetabolizing tissues	36
Liver compartment	36
Venous blood compartment	37
TCOH Submodel	38
Blood concentration	38
Body compartment	38
Liver compartment	39
TCOG Submodel	40
Blood concentration	40
Body compartment	41
Liver compartment	41
Bile compartment	41
TCA Submodel	42
Plasma binding and concentrations	42
Urinary excretion	43
Body compartment	44
Liver compartment	44
GSH conjugation submodel	45
DCA submodel	45
Likelihood function	46
<b>References</b>	<b>48</b>

**Figure S1.** Histograms of the transformed values and quantile-quantile plots for TCE metabolites TCA, DCA, DCVG and DCVC. The transformation  $y_{\text{new}}=y^{0.25}$  produced the closest average fit to normality across the metabolites, with no influential outliers.

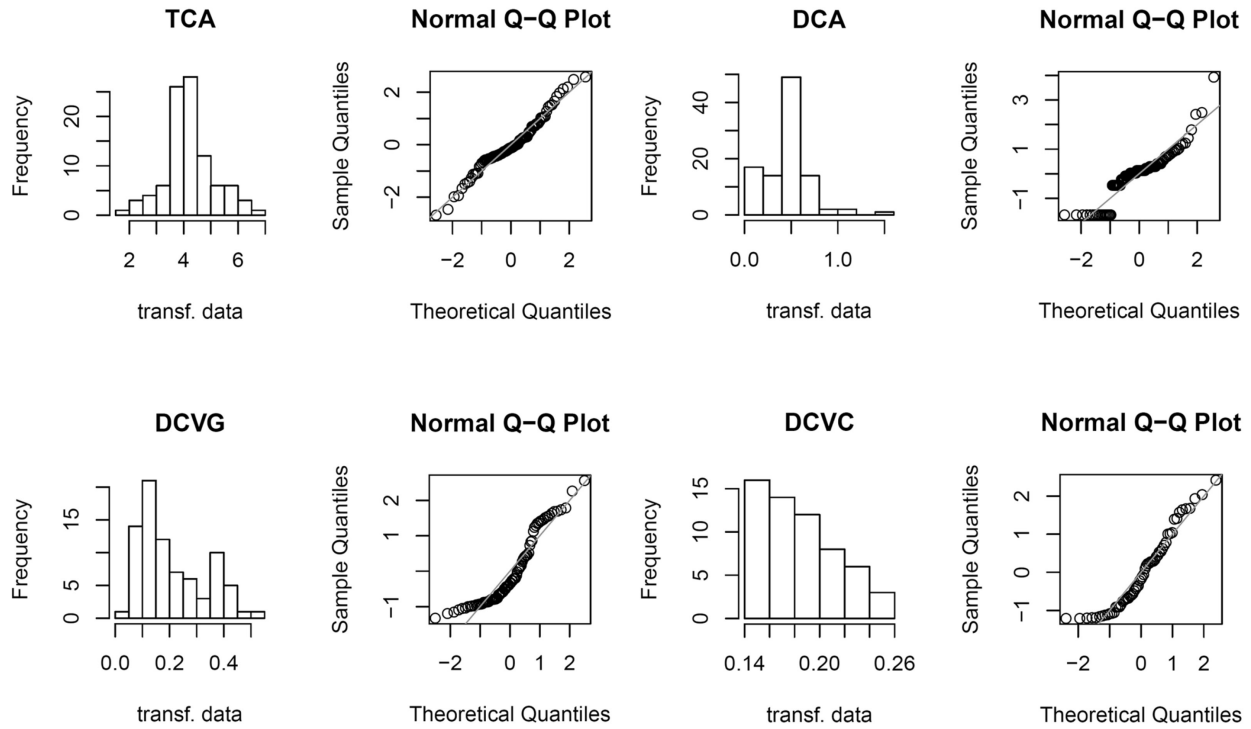


**Figure S2.** Schematic of the modified Hack et al. (2006) model. Reprinted with permission from Elsevier.

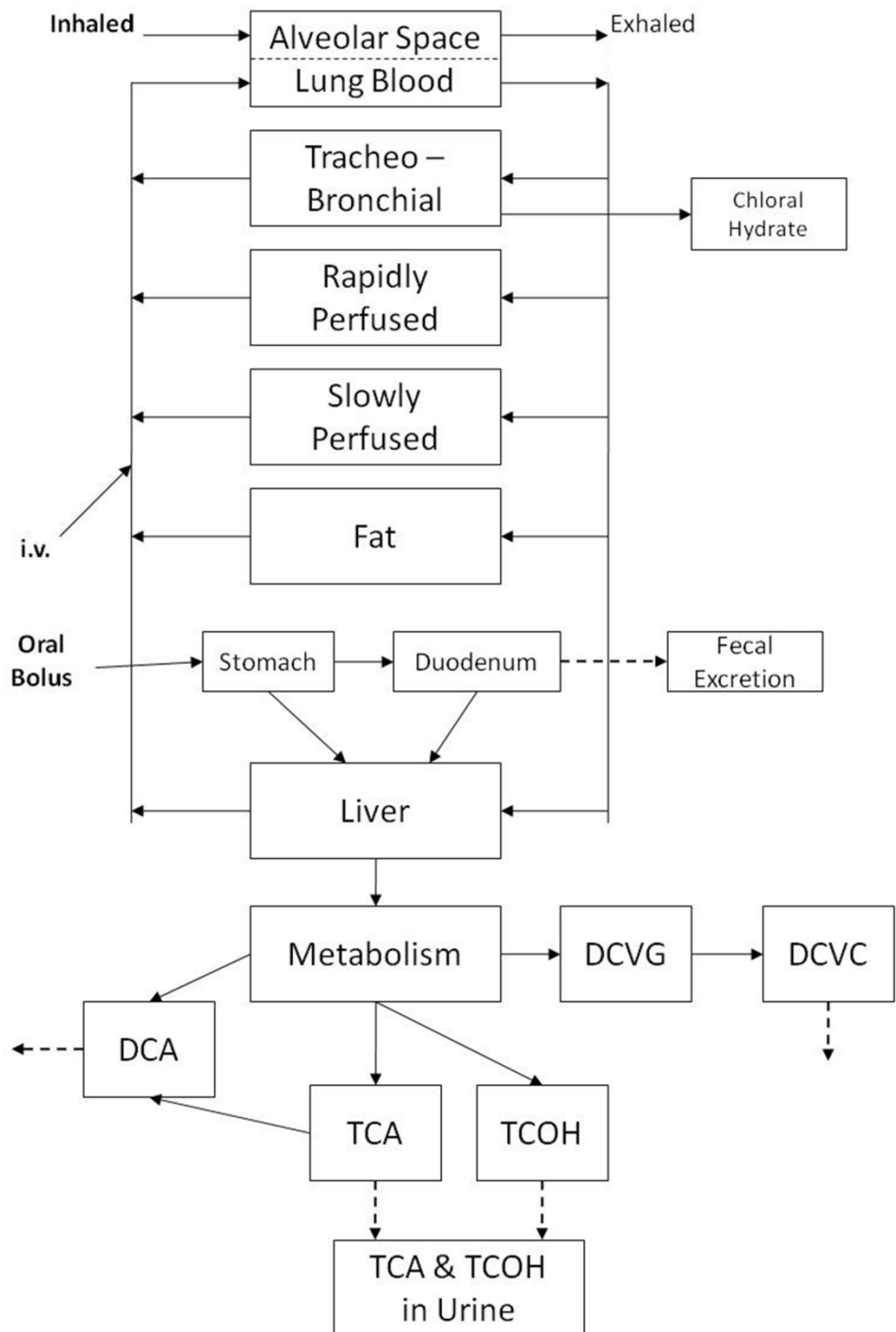


**Figure S3.** Monte Carlo simulation (100 iterations) of the multistrain mouse time-course data with the parameter distributions for metabolism and clearance of metabolites estimated to fit the range of measured values.

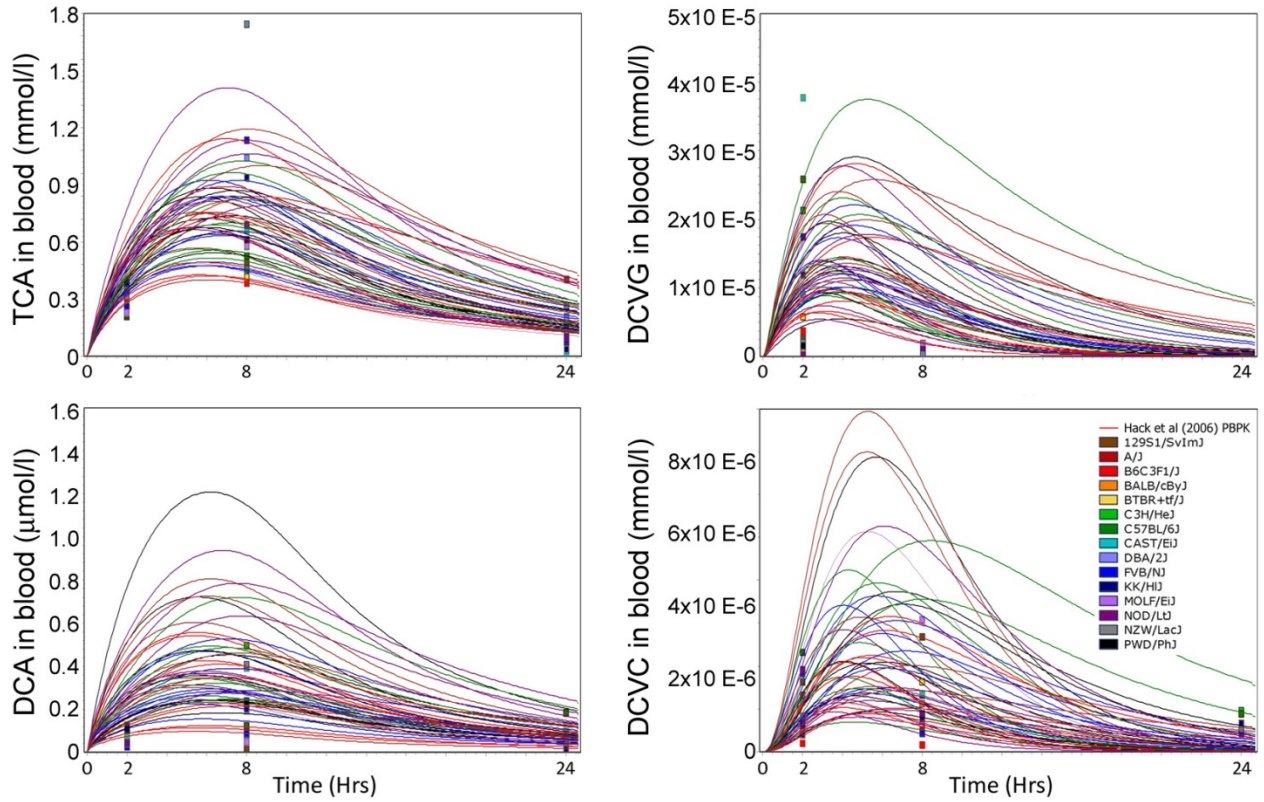


**Figure S4.** Comparison of data (solid boxes with  $\pm 1$  SD error bars) and PBPK model predictions (solid lines: interquartile range; grey area: 95% confidence interval) for TCA in mouse inbred strains [data from (Bradford et al. 2011)].

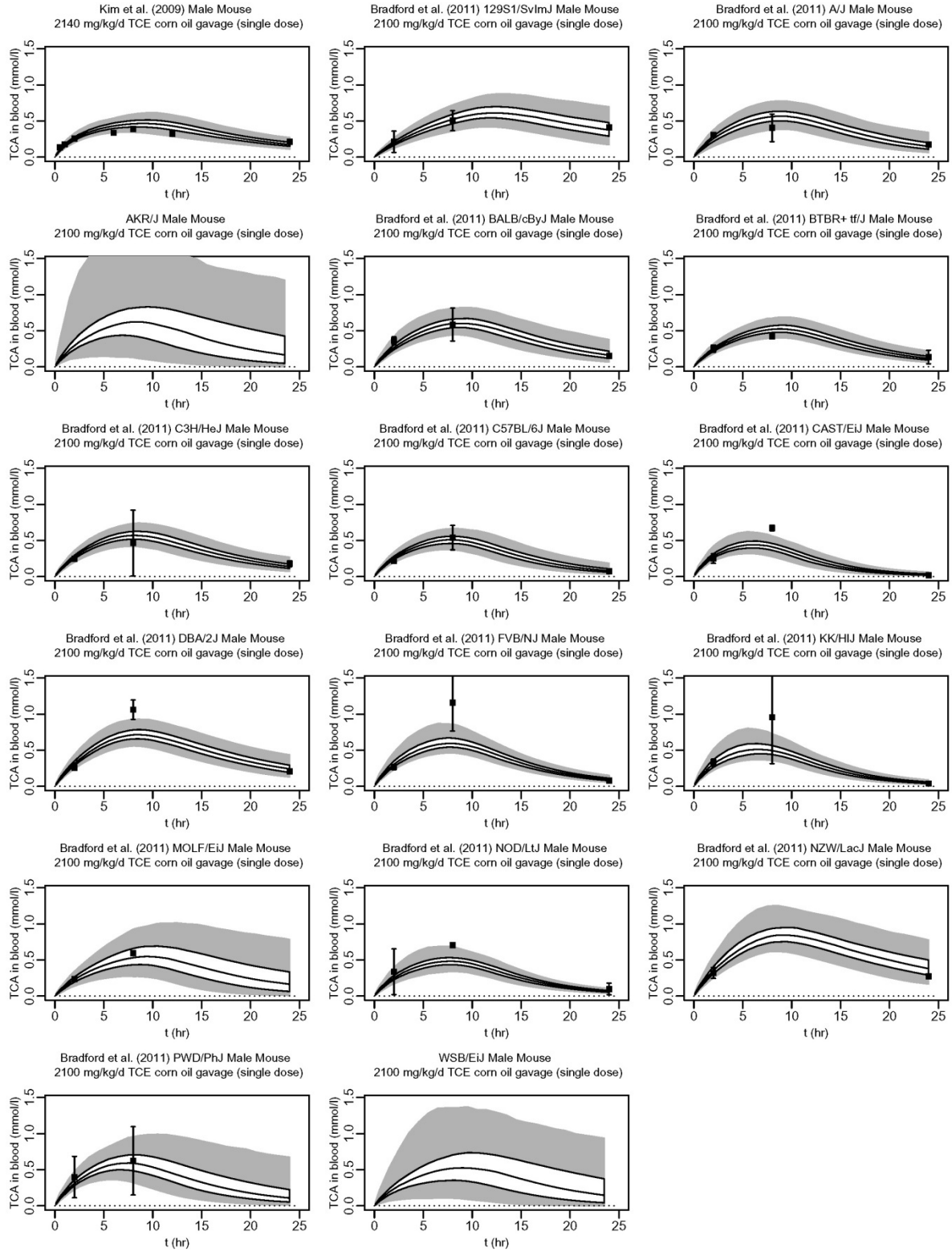


**Figure S5.** Comparison of data (solid boxes with  $\pm 1$  SD error bars) and PBPK model predictions (solid lines: interquartile range; grey area: 95% confidence interval) for DCA in mouse inbred strains [data from (Bradford et al 2011)].

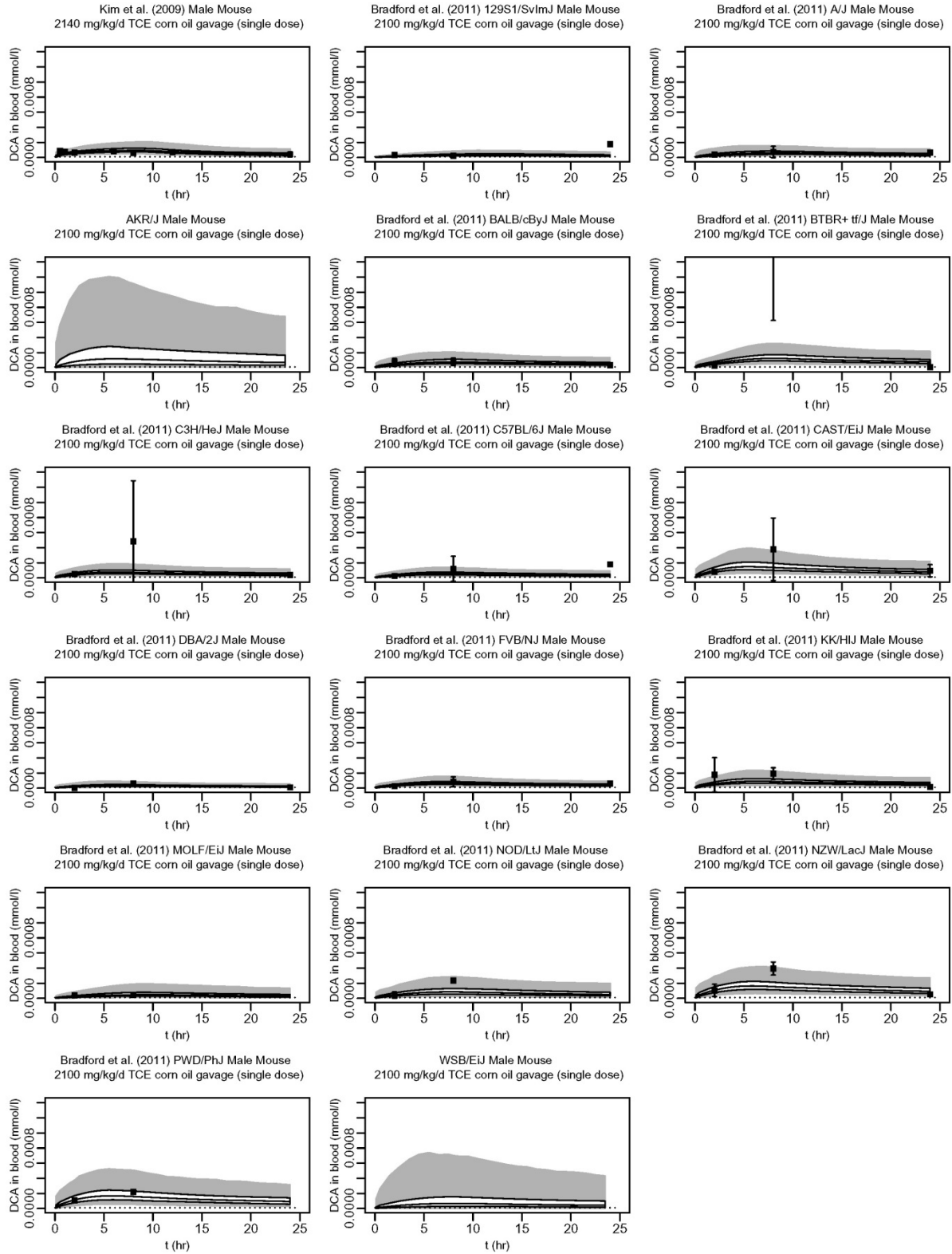


**Figure S6.** Comparison of data (solid boxes with +/- 1 SD error bars) and PBPK model predictions (solid lines: interquartile range; grey area: 95% confidence interval) for DCVG in mouse inbred strains [data from (Bradford et al 2011)].

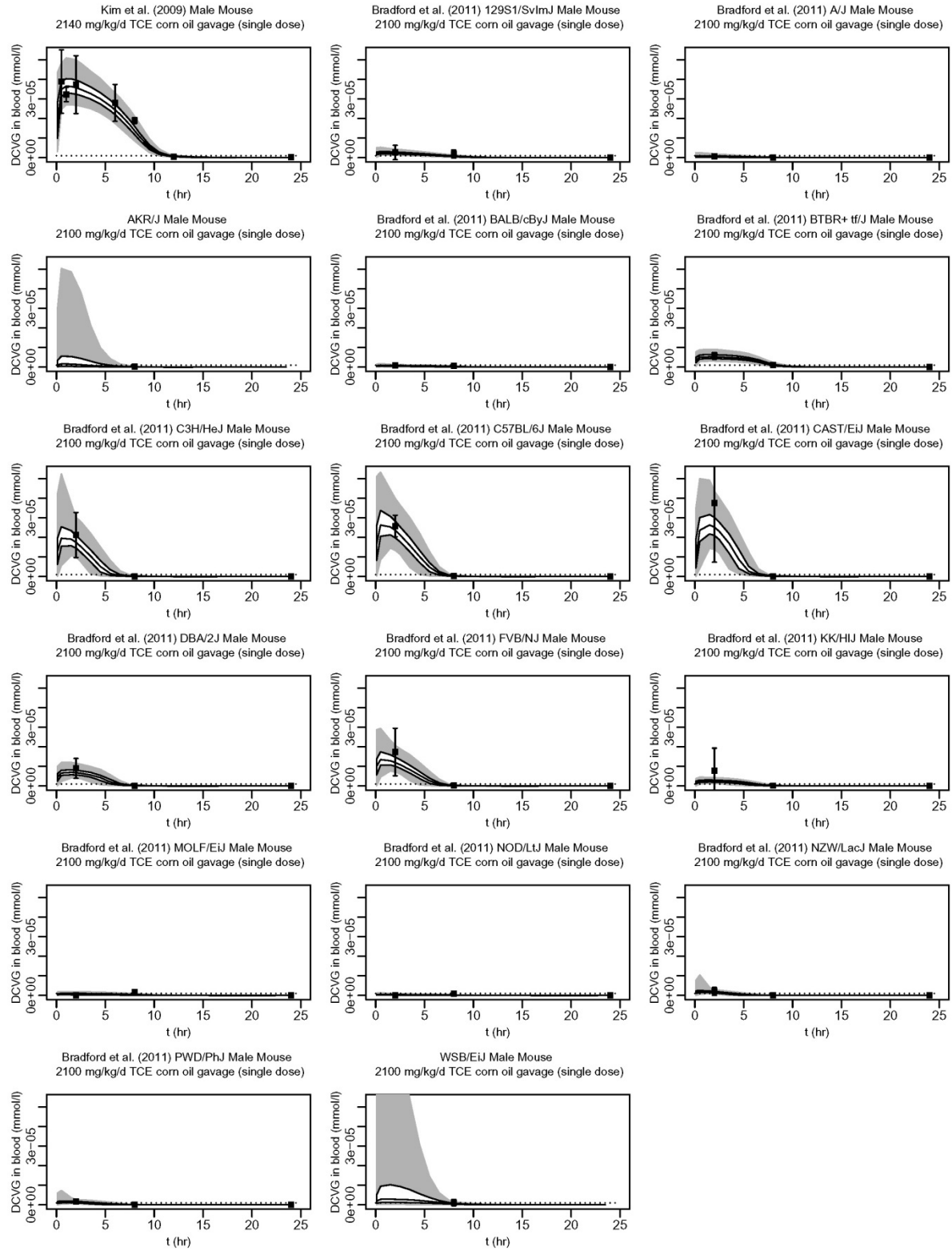


**Figure S7.** Comparison of data (solid boxes with  $\pm 1$  SD error bars) and PBPK model predictions (solid lines: interquartile range; grey area: 95% confidence interval) for DCVC in mouse inbred strains [data from (Bradford et al 2011)].

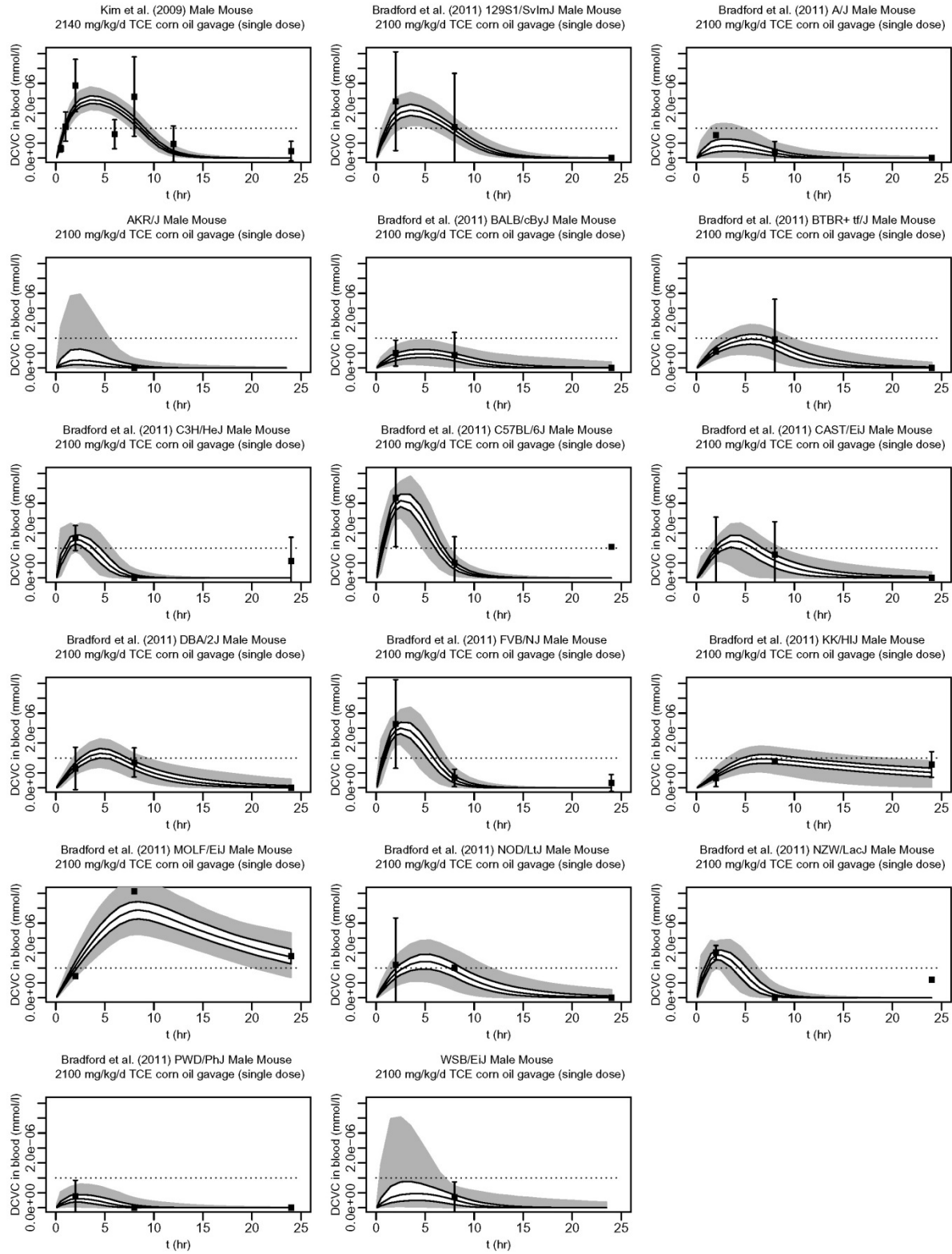


**Table S1.** TCE metabolite data for individual mice (rows) of AKR/J and WSB/EiJ strains.

<b>Strain</b>	<b>Time point (hrs)</b>	<b>Treatment</b>	<b>DCVC (nmol/ml)</b>	<b>DCVG (nmol/ml)</b>
AKR/J	8	TCE (2100 mg/kg)		5.76E-05
AKR/J	8	TCE (2100 mg/kg)		5.68E-04
AKR/J	8	Vehicle		1.77E-05
AKR/J	8	Vehicle		1.28E-04
WSB/EiJ	8	TCE (2100 mg/kg)	7.17E-04	0.00228

**Table S2.** Parameter distributions estimated with Monte Carlo analysis of the multistrain mouse data\*.

Parameter	Mean	Standard Deviation	CV
FRACTCE	0.1	0.04	0.4
KURNTCAC	0.86	0.344	0.4
FRACDCA	0.000045	0	0.4
KTCADCAC	0.00201	0.001	0.4
KCLEARDCAC	3.688	1.475	0.4
KTCEDCVGC	0.0000195	0	0.5
KDCVGDCVCC	0.204	0.102	0.5
KCLEARDCVCC	0.394	0.197	0.5

Where FRACTCE is the fractional split of TCE metabolism to TCA, KURNTCAC is the rate constant for urinary clearance of TCA, FRACDCA is the fractional split of TCE metabolism to DCA, KTCADCAC is the rate constant for TCA metabolism to DCA, KCLEARDCAC is the rate constant for clearance of DCA, KTCEDCVGC is the rate constant for TCE metabolism to DCVG, KDCVGDCVCC is the rate constant for metabolism of DCVG to DCVC, and KCLEARDCVCC is the rate constant for clearance of DCVC.

\*All parameters were distributed lognormally in the Monte Carlo simulation of the multistrain rat time-course data.

**Table S3.** PBPK model parameters, baseline values, and scaling relationships.

Model parameter: Symbol	Model parameter: Description (units)	Model parameter: Scaling formula	Scaling parameter: Symbol	Baseline value: Symbol	Baseline value: Description	Baseline value	Notes
BW	Body weight (kg)	–	–	–	–	–	a
QC	Cardiac output (L/hr)	$QC = QCC0 \times \exp(\ln QCC) \times BW^{3/4}$	lnQCC	QCC0	Cardiac output allometrically scaled	11.6	b
QP	Alveolar ventilation (L/hr)	$QP = QC \times VPR0 \times \exp(\ln VPR)$	lnVPRC	VPR0	Ventilation-perfusion ratio	2.5	c
DResp	Diffusion clearance rate (L/hr)	$DResp = QP \times \exp(\ln DRespC)$	lnDRespC	–	–	–	d
QFat	Blood flow to fat (L/hr)	$QFat = QC \times QFatC0 \times QFatC$	QFatC	QFatC0	Fraction of blood flow to fat	0.07	e
QGut	Blood flow to gut (L/hr)	$QGut = QC \times QGutC0 \times QGutC$	QGutC	QGutC0	Fraction of blood flow to gut	0.141	e
QLiv	Hepatic artery blood flow (L/hr)	$QLiv = QC \times QLivC0 \times QLivC$	QLivC	QLivC0	Fraction of blood flow to hepatic artery	0.02	e
QSlw	Blood flow to slowly perfused tissues (L/hr)	$QSlw = QC \times QSlwC0 \times QSlwC$	QSlwC	QSlwC0	Fraction of blood flow to slowly perfused tissues	0.217	e
QKid	Blood flow to kidney (L/hr)	$QKid = QC \times QKidC0 \times QKidC$	QKidC	QKidC0	Fraction of blood flow to kidney	0.091	e
QRap	Blood flow to rapidly perfused tissues (L/hr)	$QRap = QC - (QFat + QGut + QLiv + QSlw + QKid)$	–	–	–	–	e
FracPlas	Fraction of blood that is plasma	$FracPlas = FracPlas0 \times FracPlasC$	FracPlasC	FracPlas0	Fraction of blood that is plasma	0.52	f
VFat	Volume of fat (L)	$VFat = BW \times VFatC0 \times VFatC$	VFatC	VFatC0	Fraction of body weight that is fat	0.07	g

Model parameter: Symbol	Model parameter: Description (units)	Model parameter: Scaling formula	Scaling parameter: Symbol	Baseline value: Symbol	Baseline value: Description	Baseline value	Notes
VGut	Volume of gut (L)	$VGut = BW \times VGutC0 \times VGutC$	VGutC	VGutC0	Fraction of body weight that is gut	0.049	g
VLiv	Volume of liver (L)	$VLiv = BW \times VLivC0 \times VLivC$	VLivC	VLivC0	Fraction of body weight that is liver	0.055	g
VRap	Volume of rapidly perfused tissues (L)	$VRap = BW \times VRapC0 \times VRapC$	VRapC	VRapC0	Fraction of body weight that is rapidly perfused	0.1	g
VRespLum	Volume of respiratory tract lumen (L)	$VRespLum = BW \times VRespLumC0 \times VRespLumC$	VRespLumC	VRespLumC0	Respiratory lumen volume as fraction body weight	0.004667	g
VResp	Volume of respiratory tract tissue (L)	$VResp = BW \times VRespC0 \times VRespC$	VRespC	VRespC0	Fraction of body weight that is respiratory tract	0.0007	g
VRespEff	Effective air volume of respiratory tract tissue	$VRespEff = VResp \times PResp \times PB$	—	—	—	—	g
VKid	Volume of kidney (L)	$VKid = BW \times VKidC0 \times VKidC$	VKidC	VKidC0	Fraction of body weight that is kidney	0.017	g
VBld	Volume of blood (L)	$VBld = BW \times VBldC0 \times VBldC$	VBldC	VBldC0	Fraction of body weight that is blood	0.049	g
VSlw	Volume of slowly perfused tissue (L)	$VSlw = BW \times VperfC0 - (VFat + VGut + VLiv + VRap + VResp + VKid + VBld)$	—	VperfC0	Fraction of body weight that is blood perfused	0.8897	g
VPlas	Volume of plasma (L)	$VPlas = FracPlas \times VBld$	—	—	—	—	h
VBod	Volume body for TCA submodel (L)	$VBod = VFat + VGut + VRap + VResp + VKid + VSlw$	—	—	—	—	i

Model parameter: Symbol	Model parameter: Description (units)	Model parameter: Scaling formula	Scaling parameter: Symbol	Baseline value: Symbol	Baseline value: Description	Baseline value	Notes
VBodTCOH	Volume body for TCOH and TCOG submodels (L)	VBodTCOH = VBod + VBld	-	-	-	-	j
PB	TCE blood-air partition coefficient	PB=PB0×PBC	PBC	PB0	TCE blood-air partition coefficient	15	k
PFat	TCE fat-blood partition coefficient	PFat=PFatC0×exp(PFatC)	PFatC	PFatC0	TCE fat-blood partition coefficient	36	l
PGut	TCE gut-blood partition coefficient	PGut=(PGutC0)×exp(lnPGutC)	lnPGutC	PGutC0	TCE gut-blood partition coefficient	1.9	m
PLiv	TCE liver-blood partition coefficient	PLiv = (PLivC0) × exp(lnPLivC)	lnPLivC	PLivC0	TCE liver-blood partition coefficient	1.7	n
PRap	TCE rapidly perfused-blood partition coefficient	PRap = (PRapC0) × exp(lnPRapC)	lnPRapC	PRapC0	TCE rapidly perfused-blood partition coefficient	1.9	o
PResp	TCE respiratory tract tissue-blood partition coefficient	Presp = (PRespC0) × exp(lnPRespC)	lnPRespC	PRespC0	TCE respiratory tract tissue-blood partition coefficient	2.6	p
PKid	TCE kidney-blood partition coefficient	PKid = (PKidC0) × exp(lnPKidC)	lnPKidC	PKidC0	TCE kidney-blood partition coefficient	2.1	q
PSlw	TCE slowly perfused-blood partition coefficient	PSlw = (PSlwC0) × exp(lnPSlwC)	lnPSlwC	PSlwC0	TCE slowly perfused-blood partition coefficient	2.4	r
TCAPlas	TCA blood-plasma concentration ratio	TCAPlas = FracPlas + (1 – FracPlas) × PRBCPlasTCA0 × exp(lnPRBCPlasTCAC)	InPRBCPlasTCAC	PRBCPlasTCA0	TCA red blood cell-plasma partition coefficient	0.5	s

Model parameter: Symbol	Model parameter: Description (units)	Model parameter: Scaling formula	Scaling parameter: Symbol	Baseline value: Symbol	Baseline value: Description	Baseline value	Notes
PBodTCA	Free TCA body-plasma partition coefficient	$PBodTCA = TCAPlas \times PBodTCAC0 \times \exp(\lnPBodTCAC)$	$\lnPBodTCAC$	$PBodTCAC0$	Free TCA body-blood partition coefficient	0.88	t
PLivTCA	Free TCA liver-plasma partition coefficient	$PLivTCA = TCAPlas \times PLivTCAC0 \times \exp(\lnPLivTCAC)$	$\lnPLivTCAC$	$PLivTCAC0$	Free TCA liver-blood partition coefficient	1.18	t
kDissoc	Protein TCA dissociation constant (microM)	$kDissoc = kDissoc0 \times \exp(\lnkDissocC)$	$\lnkDissocC$	$kDissoc0$	Protein TCA dissociation constant (microM)	107	u
BMax	Protein concentration (microM)	$BMax = BMaxkD0 \times kDissoc \times \exp(\lnBMaxkDC)$	$\lnBMaxkDC$	$BMaxkD0$	BMax/kDissoc ratio	0.88	u
PBodTCOH	TCOH body-blood partition coefficient	$PBodTCOH = PBodTCOH0 \times \exp(\lnPBodTCOHC)$	$\lnPBodTCOHC$	$PBodTCOH0$	TCOH body-blood partition coefficient	1.11	v
PLivTCOH	TCOH liver-blood partition coefficient	$PBodTCOH = PLivTCOH0 \times \exp(\lnPLivTCOHC)$	$\lnPLivTCOHC$	$PLivTCOH0$	TCOH liver-blood partition coefficient	1.3	v
PBodTCOG	TCOG body-blood partition coefficient	$PBodTCOG = PBodTCOG0 \times \exp(\lnPBodTCOGC)$	$\lnPBodTCOGC$	$PBodTCOG0$	TCOG body-blood partition coefficient	1.11	w
PLivTCOG	TCOG liver-blood partition coefficient	$PBodTCOG = PLivTCOG0 \times \exp(\lnPLivTCOGC)$	$\lnPLivTCOGC$	$PLivTCOG0$	TCOG liver-blood partition coefficient	1.3	w
VDCVG	DCVG distribution volume (L)	$VDCVG = VBld + (VBod+VLiv) \times \exp(\lnPeffDCVG)$	$\lnPeffDCVG$	—	—	—	x
VDCVC	DCVC distribution volume (L)	$VDCVC = VBld + (VBod+VLiv) \times \exp(\lnPeffDCVC)$	$\lnPeffDCVC$	—	—	—	x

Model parameter: Symbol	Model parameter: Description (units)	Model parameter: Scaling formula	Scaling parameter: Symbol	Baseline value: Symbol	Baseline value: Description	Baseline value	Notes
VDCA	DCA distribution volume (L)	$VDCA = VBld + (VBod+VLiv) \times \exp(\lnPeffDCA)$	$\lnPeffDCA$	-	-	-	x
VMAX	VMAX for TCE hepatic oxidation (mg/hr)	$VMAX = VMAX0 \times VLiv \times \exp(\lnVMAXC)$	$\lnVMAXC$	$VMAX0$	VMAX per kg liver for TCE hepatic oxidation (mg/hr/kg liver)	2,700	y
KM	KM for TCE hepatic oxidation (mg/L blood)	$KM = KM0 \times \exp(\lnKMC)$	$\lnKMC$	$KM0$	KM for TCE hepatic oxidation (mg/L)	36	y
FracOther	Fraction of TCE oxidation not to TCA or TCOH	$FracOther = \exp(\lnFracOtherC) / (1+\exp(\lnFracOtherC))$	$\lnFracOtherC$	-	-	-	z
FracTCA	Fraction of TCE oxidation to TCA	$FracTCA = (1-FracOther) \times \logitFracTCA0 \times \exp(\lnFracTCAC) / (1 + \logitFracTCA0 \times \exp(\lnFracTCAC))$	$\lnFracTCAC$	$\logitFracTCA0$	Log of ratio of fraction to TCA to fraction not to TCA	0.32	aa
VMAXDCVG	VMAX for TCE hepatic GSH conjugation (mg/hr)	$VMAXDCVG = VMAXDCVG0 \times VLiv \times \exp(\lnVMAXDCVGC)$	$\lnVMAXDCVGC$	$VMAXDCVG0$	VMAX per kg liver for TCE GSH conjugation (mg/hr/kg liver)	300	bb
KMDCVG	KM for TCE hepatic GSH conjugation (mg/L blood)	$KMDCVG = VMAXDCVG / (ClDCVG0 \times \exp(\lnClDCVGC))$	$\lnClDCVGC$	$ClDCVG0$	VMAX/KM per kg liver for TCE hepatic GSH conjugation (L blood/hr/kg liver)	1.53	bb
KMClara	KM for TCE lung oxidation (mg/L air)	$KMClara = \exp(\lnKMClara)$	-	-	-	-	cc

Model parameter: Symbol	Model parameter: Description (units)	Model parameter: Scaling formula	Scaling parameter: Symbol	Baseline value: Symbol	Baseline value: Description	Baseline value	Notes
VMAXClara	VMAX for TCE lung oxidation (mg/hr)	$VMAXClara = VMAX \times VMAXLungLiv0 \times \exp(\lnVMAXLungLivC)$	$\lnVMAXLungLivC$	$VMAXLungLiv0$	Ratio of lung to liver total VMAX (mg/hr per mg/hr)	0.07	cc
FracLungSys	Fraction of respiratory oxidation entering systemic circulation	$FracLungSys = \exp(\lnFracLungSysC)/(1 + \exp(\lnFracLungSysC))$	$\lnFracLungSysC$	—	—	—	dd
VMAXTCOH	VMAX for TCOH oxidation to TCA (mg/hr)	$VMAXTCOH = BW^{1/4} \times \exp(\lnVMAXTCOHC)$	$\lnVMAXTCOHC$	—	—	—	
KMTCOH	KM for TCOH oxidation to TCA (mg/L air)	$KMTCOH = \exp(\lnKMTCOHC)$	$\lnKMTCOHC$	—	—	—	
VMAXGluc	VMAX for TCOH glucuronidation (mg/hr)	$VMAXGluc = BW^{1/4} \times \exp(\lnVMAXGlucC)$	$\lnVMAXGlucC$	—	—	—	
KMGluc	KM for TCOH glucuronidation (mg/L air)	$KMGluc = \exp(\lnKMGlucC)$	$\lnKMGlucC$	—	—	—	
kMetTCOH	Rate constant for TCOH other clearance (/hr)	$kMetTCOH = BW^{-1/4} \times \exp(\lnkMetTCOHC)$	$\lnkMetTCOHC$	—	—	—	
kUrnTCA	Rate constant for TCA excretion to urine (/hr)	$kUrnTCA = GFR\_BW \times \exp(\lnkUrnTCAC) \times BW / VPlas$	$\lnkUrnTCAC$	$GFR\_BW$	Glomerular filtration rate per kg body weight (L/h/kg)	0.6	ee
kMetTCA	Rate constant for other TCA clearance (/hr)	$kMetTCA = BW^{-1/4} \times \exp(\lnkMetTCAC)$	$\lnkMetTCAC$	—	—	—	
kBile	Rate constant for other TCOG excretion to bile (/hr)	$kBile = BW^{-1/4} \times \exp(\lnkBileC)$	$\lnkBileC$	—	—	—	

Model parameter: Symbol	Model parameter: Description (units)	Model parameter: Scaling formula	Scaling parameter: Symbol	Baseline value: Symbol	Baseline value: Description	Baseline value	Notes
kEHR	Rate constant for other bile TCOG reabortion as TCOH (/hr)	$kEHR = BW^{-1/4} \times \exp(\ln kEHRC)$	lnkEHRC	-	-	-	
kUrnTCOG	Rate constant for TCOH excretion to urine (/hr)	$kUrnTCOG = GFR\_BW \times \exp(\ln kUrnTCOGC) \times BW / (VBodTCOH \times PBodTCOG)$	lnkUrnTCOGC	GFR_BW	Glomerular filtration rate per kg body weight (L/hr/kg)	0.6	ee
kDCVG	Rate constant for DCVC formation from DCVG (/hr)	$kDCVG = BW^{-1/4} \times \exp(\ln kDCVGC)$	lnkDCVGC	-	-	-	
kElimDCVC	Lumped rate constant for elimination of DCVC (/hr)	$kElimDCVC = BW^{-1/4} \times \exp(\ln kElimDCVCC)$	lnkElimDCVCC	-	-	-	
kClearDCVC	Rate constant for clearance of DCA (/hr)	$kClearDCA = BW^{-1/4} \times \exp(\ln kClearDCAC)$	lnkClearDCAC	-	-	-	
kDCAcen_per	Rate constant for DCA central-to-peripheral (/hr)	$kDCAcen\_per = BW^{-1/4} \times \exp(\ln kDCAcen\_perc)$	lnkDCAcen_perC	-	-	-	
kDCAper_cen	Rate constant for DCA peripheral-to-central (/hr)	$kDCAper\_cen = BW^{-1/4} \times \exp(\ln kDCAper\_cenC)$	lnkDCAper_cenC	-	-	-	
kTSD	TCE gavage stomach-duodenum transfer coefficient (/hr)	$kTSD = \exp(\ln kTSD)$	lnkTSD	-	-	-	ff
kAS	TCE gavage stomach-absorption coefficient (/hr)	$kAS = \exp(\ln kAS)$	lnkAS	-	-	-	ff
kAD	TCE gavage duodenum-absorption coefficient (/hr)	$kAD = \exp(\ln kAD)$	lnkAD	-	-	-	ff

Model parameter: Symbol	Model parameter: Description (units)	Model parameter: Scaling formula	Scaling parameter: Symbol	Baseline value: Symbol	Baseline value: Description	Baseline value	Notes
kASTCA	TCA stomach absorption coefficient (/hr)	$k_{ASTCA} = \exp(\ln k_{ASTCA})$	$\ln k_{ASTCA}$	-	-	-	ff
kASTCOH	TCOH stomach absorption coefficient (/hr)	$k_{ASTCOH} = \exp(\ln k_{ASTCOH})$	$\ln k_{ASTCOH}$	-	-	-	ff

Explanatory note: "Scaling parameters" are the parameters which may be given an uncertainty distribution in the statistical analysis. See Table S1 for the prior distributions for these parameters. For fixed parameters, see the notes below.

Notes: <sup>a</sup>Use measured value if available. Otherwise assume BW = 0.03 kg. <sup>b</sup>Baseline values are from Brown et al. (1997). <sup>c</sup>Scale by QC using alveolar VPR. Baseline values are from Brown et al. (1997). <sup>d</sup>Scaling parameter is relative to alveolar ventilation rate. <sup>e</sup>Fat represents adipose tissue only. Gut is the GI tract, pancreas, and spleen (all drain to the portal vein). Slowly perfused tissue is the muscle and skin. Rapidly perfused tissue is the rest of the organs, plus the bone marrow and lymph nodes, the blood flow for which is calculated as the difference between the cardiac output (QC) and the sum of the other blood flows. Baseline values are from Brown et al. (1997). Scaling parameter fixed at 1. <sup>f</sup>This is equal to 1 minus the hematocrit (measured value used if available). Baseline values from control animals in (Hejtmancik et al. 2002). Scaling parameter fixed at 1. <sup>g</sup>Fat represents adipose tissue only, and the measured value is used, if available. Gut is the GI tract, pancreas, and spleen (all drain to the portal vein). Rapidly perfused tissue is the rest of the organs, plus the bone marrow and lymph nodes, minus the tracheobronchial region. The respiratory tissue volume is tracheobronchial region, with an effective air volume given by multiplying by its tissue:air partition coefficient (= tissue:blood times blood:air). The slowly perfused tissue is the muscle and skin. This leaves a small (10–15% of body weight) unperfused volume that consists mostly of bone (minus marrow) and the GI tract contents. Baseline values are from Brown et al. (1997), except for volumes of the respiratory lumen, which are from Sarangapani et al. (2003). Scaling parameter fixed at 1. <sup>h</sup>Derived from blood volume using FracPlas. <sup>i</sup>Sum of all compartments except the blood and liver. <sup>j</sup>Sum of all compartments except the liver. <sup>k</sup>Pooling Abbas and Fisher (1997) and Fisher et al. (1991). Scaling parameter fixed at 1. <sup>l</sup>Abbas and Fisher (1997). Scaling parameter fixed at 1. <sup>m</sup>Value is the geometric mean of liver and kidney (relatively high uncertainty) values. Scaling parameter fixed at 0. <sup>n</sup>Fisher et al. (1991). Scaling parameter fixed at 0. <sup>o</sup>Geometric mean of liver and kidney values. Scaling parameter fixed at 0. <sup>p</sup>Lung value from Abbas and Fisher (1997). Scaling parameter fixed at 0. <sup>q</sup> Abbas and Fisher (1997). Scaling parameter fixed at 0. <sup>r</sup>Muscle value from Abbas and Fisher (1997). Scaling parameter fixed at 0. <sup>s</sup>Scaling parameter is the effective partition coefficient between red blood cells and plasma. Thus, the TCA blood-plasma concentration ratio depends on the plasma fraction. Baseline value is based on the blood-plasma concentration ratio of 0.76 in rats (Schultz et al. 1999). <sup>t</sup>In vitro partition coefficients were determined at high concentration, when plasma binding is saturated, so should reflect the free blood:tissue partition coefficient. To get the plasma partition coefficient, the partition coefficient is multiplied by the blood:plasma concentration ratio (TCAPlas). In vitro values were

from Abbas and Fisher (1997). Body values based on measurements in muscle. Scaling parameter fixed at 0. <sup>w</sup>Values are based on the geometric mean of estimates based on data from Lumpkin et al. (2003), Schultz et al. (1999), Templin et al. (1993; 1995), and Yu et al. (2000). Scaling parameter for BMAX is actually the ratio of BMAX/kD, which determines the binding at low concentrations. <sup>v</sup>Data are from Abbas and Fisher (1997). Scaling parameter fixed at 0. <sup>w</sup>Used in vitro measurements in TCOH as a proxy, but higher uncertainty is noted. Scaling parameter fixed at 0. <sup>x</sup>The scaling parameter is the effective partition coefficient for the “body” (nonblood) compartment, so that the distribution volume for X ( $V_X$ ) is given by  $VBld + \exp(\lnPeff_X) \times (VBod + VLiv)$ . <sup>y</sup>Baseline values have the following units: for VMAX, mg/hr/kg liver; for KM, mg/L blood; and for clearance (Cl), L/hr/kg liver. Values are based on in vitro (microsomal and hepatocellular preparations) from Elfarra et al. (1998), Lipscomb et al. (1998a; 1997, 1998b). Scaling from in vitro data based on 32 mg microsomal protein/g liver and  $99 \times 10^6$  hepatocytes/g liver (Barter et al. 2007). Scaling of KM from microsomes were based on two methods: (1) assuming microsomal concentrations equal to liver tissue concentrations and (2) using the measured microsome:air partition coefficient and a central estimate of the blood:air partition coefficient. <sup>z</sup>Scaling parameter is ratio of “DCA” to “non-DCA” oxidative pathway (where DCA is a proxy for oxidative metabolism not producing TCA or TCOH). Fraction of “other” oxidation is  $\exp(\lnFracOtherC)/(1 + \exp[\lnFracOtherC])$ . <sup>aa</sup>Scaling parameter is ratio of TCA to TCOH pathways. Baseline value based on geometric mean of Lipscomb et al. (1998a) using fresh hepatocytes and Bronley-DeLancey et al. (2006) using cryogenically-preserved hepatocytes. Fraction of oxidation to TCA is  $(1 - FracOther) \times \exp(\lnFracTCAC)/(1 + \exp[\lnFracTCAC])$ . <sup>bb</sup>Baseline values are based on in vitro data at 1 or 2 mM (Lash et al. 1998; Lash et al. 1995). In most cases, rates at 2 mM were increased over the same sex/species at 1 mM, indicating VMAX has not yet been reached. These data therefore put lower bounds on both VMAX (in units of mg/hr/kg tissue) and clearance (in units of L/hr/kg tissue), so those are the scaling parameters used, with those bounds used as baseline values. <sup>cc</sup>Scaling parameter is the ratio of the lung to liver VMAX (each in units of mg/hr), with baseline values based on microsomal preparations (mg/hr/mg protein) assayed at  $\sim 1$  mM (Green et al. 1997), further adjusted by the ratio of lung to liver tissue masses (Brown et al. 1997; Publication 89, ICRP 2003). <sup>dd</sup>Scaling parameter is the ratio of respiratory oxidation entering systemic circulation (translocated to the liver) to that locally cleared in the lung. Fraction of respiratory oxidation entering systemic circulation is  $\exp(\lnFracLungSysC)/(1 + \exp[\lnFracLungSysC])$ . <sup>ee</sup>Baseline parameters for urinary clearance (L/hr) were based on glomular filtration rate per unit body weight (L/hr/kg body weight) from Lin (1995), multiplied by the body weights cited in the study. For TCA, these were scaled by plasma volume to obtain the rate constant (/hr), since the model clears TCA from plasma. For TCOG, these were scaled by the effective distribution volume of the body ( $VBodTCOH \times PBodTCOG$ ) to obtain the rate constant (/hr), since the model clears TCOG from the body compartment. <sup>ff</sup>Baseline value for oral absorption scaling parameter are as follows: kTSD and kAS, 1.4/hr, based on human stomach half time of 0.5 hr; kAD, kASTCA, and kASTCOH, 0.75/hr, based on human small intestine transit time of 4 hrs (Publication 89, ICRP 2003). These are noted to have very high uncertainty.

**Table S4.** Uncertainty distributions for the population mean and variance of the PBPK model parameters.

Scaling parameter	Population mean: Distribution	Population mean: SD or Min	Population mean: Truncation ( $\pm$ nxSD) or Max	Population mean: Notes	Population variance: CV	Population variance: CU	Population variance: Notes
lnQCC	TruncNormal	0.2	4	a	0.2	2	aa
lnVPRC	TruncNormal	0.2	4	a	0.2	2	aa
lnDRespC	Uniform	-11.513	2.303	b	0.2	0.5	aa
lnPRBCPlasTCAC	Uniform	-4.605	4.605	c	0.336	2	bb
lnkDissocC	TruncNormal	1.191	3	d	1.191	2	cc
lnBMaxkDC	TruncNormal	0.495	3	d	0.495	2	cc
lnPeffDCVG	Uniform	-6.908	6.908	e	0.4	2	cc
lnPeffDCVC	Uniform	-6.908	6.908	e	0.4	2	cc
lnPeffDCA	Uniform	-6.908	6.908	e	0.4	2	cc
lnVMAXC	TruncNormal	0.693	3	f	0.824	1	dd
lnKMC	TruncNormal	1.386	3	f	0.270	1	dd
lnFracOtherC	Uniform	-6.908	6.908	e	0.5	2	ee
lnFracTCAC	TruncNormal	1.163	3	g	0.5	2	ee
lnVMAXDCVGC	Uniform	-6.908	6.908	h	0.5	2	ee
lnClDCVGC	Uniform	-6.908	6.908	h	0.5	2	ee

Scaling parameter	Population mean: Distribution	Population mean: SD or Min	Population mean: Truncation ( $\pm$ nxSD) or Max	Population mean: Notes	Population variance: CV	Population variance: CU	Population variance: Notes
lnVMAXLungLivC	TruncNormal	1.099	3	i	0.5	2	ee
lnKMClera	Uniform	-6.908	6.908	e	0.5	2	ee
lnFracLungSysC	Uniform	-6.908	6.908	e	0.5	2	ee
lnVMAXTCOHC	Uniform	-9.21	9.21	e	0.5	2	ee
lnKMTCOH	Uniform	-9.21	9.21	e	0.5	2	ee
lnVMAXGlucC	Uniform	-9.21	9.21	e	0.5	2	ee
lnKMGluc	Uniform	-6.908	6.908	e	0.5	2	ee
lnkMetTCOHC	Uniform	-11.513	6.908	e	0.5	2	ee
lnkUrnTCAC	Uniform	-4.605	4.605	e	0.5	2	ee
lnkMetTCAC	Uniform	-9.21	4.605	e	0.5	2	ee
lnkBileC	Uniform	-9.21	4.605	e	0.5	2	ee
lnkEHRC	Uniform	-9.21	4.605	e	0.5	2	ee
lnkUrnTCOGC	Uniform	-6.908	6.908	e	0.5	2	ee
lnkDCVGC	Uniform	-9.21	4.605	e	0.5	2	ee
lnkElimDCVCC	Uniform	-9.21	4.605	e	0.5	2	ee
lnkClearDCAC	Uniform	-9.21	4.605	e	0.5	2	ee

Scaling parameter	Population mean: Distribution	Population mean: SD or Min	Population mean: Truncation ( $\pm nxSD$ ) or Max	Population mean: Notes	Population variance: CV	Population variance: CU	Population variance: Notes
lnkDCAcen_perC	Uniform	-9.21	4.605	e	0.5	2	ee
lnkDCAper_cenC	Uniform	-9.21	4.605	e	0.5	2	ee
lnkTSD	Uniform	-4.269	4.942	e	2	2	ff
lnkAS	Uniform	-6.571	7.244	e	2	2	ff
lnkAD	Uniform	-7.195	6.62	e	2	2	ff
lnkASTCA	Uniform	-7.195	6.62	e	2	2	ff
lnkASTCOH	Uniform	-7.195	6.62	e	2	2	ff

Explanatory note: All population mean parameters have either truncated normal (TruncNormal) or uniform distributions. For those with TruncNormal distributions, the mean for the population mean is 0 for natural-log transformed parameters (parameter name starting with “ln”) and one for untransformed parameters, with the truncation at the specified number (n) of SDs. All uniformly distributed parameters are natural-log transformed, so their untransformed minimum and maximum are exp(Min) and exp(Max), respectively. All population variance parameters (V\_pname, for parameter “pname”) have Inverse-Gamma distributions, with the expected value given by CV and coefficient of uncertainty given by CU (i.e., SD of V\_pname divided by expected value of V\_pname) (notation the same as Hack et al. 2006). Under these conditions, the Inverse-Gamma distribution has a shape parameter is given by  $\alpha = 2 + 1/CU^2$  and scale parameter  $\beta = (\alpha - 1) CV^2$ . In addition, it should be noted that, under a normal distribution and a uniform prior distribution on the population variance, the posterior distribution for the variance given  $n$  data points with a sample variance  $s^2$  is given by an Inverse-Gamma distribution with  $\alpha = (n - 1)/2$  and  $\beta = \alpha s^2$ . Therefore, the “effective” number of data points is given by  $n = 5 + 2/CU^2$  and the “effective” sample variance is  $s^2 = CV^2 \alpha / (\alpha - 1)$ .

Notes: <sup>a</sup>Uncertainty based on coefficient of variation (CV) or range of values in Brown et al. (1997). <sup>b</sup>Noninformative prior distribution intended to span a wide range of possibilities because no independent data are available on these parameters. <sup>c</sup>No in vitro data was available, so a noninformative prior was used. <sup>d</sup>GSD for uncertainty based on different estimates from different in vitro studies. <sup>e</sup>Noninformative prior

distribution. <sup>f</sup>Assume twofold uncertainty GSD in VMAX, based on observed variability and uncertainties of in vitro-to-in vivo scaling. For KM, the uncertainty is assumed to be fourfold, due to the different methods for scaling of concentrations from TCE in the in vitro medium to TCE in blood. <sup>g</sup>Uncertainty GSD of 3.2-fold reflects difference between in vitro measurements from Lipscomb et al. (1998a) and Bronley-DeLancey et al. (2006). <sup>h</sup>The baseline values are notional lower-limits on VMAX and clearance; however, the lower bound of the prior distribution is set to 100-fold less because of uncertainty in in vitro-in vivo extrapolation, and because Green et al. (1997) reported values 100-fold smaller than Lash et al. (1998; 1995). <sup>i</sup>Uncertainty GSD of threefold was assumed due to possible differences in microsomal protein content, the fact that measurements were at a single concentration, and the fact that the human baseline values was based on the limit of detection. <sup>aa</sup>CV values generally taken to be equal to the uncertainty SD in the population mean, most of which were based on variability between studies (i.e., not clear whether variability represents uncertainty or variability). Given this uncertainty, CU of 2 assigned to cardiac output and ventilation-perfusion, while CU of 0.5 assigned to the remaining physiological parameters. <sup>bb</sup>Used value from uncertainty in population in mean in rats for all species with high uncertainty. <sup>cc</sup>It is not clear whether interstudy variability is due to intersubject or assay variability, so the same central were assigned to the uncertainty in the population mean as to the central estimate of the population variance. In the cases where direct measurements were available, the CU for the uncertainty in the population variance is based on the actual sample n, with the derivation discussed in the notes preceding this table. Otherwise, a CU of 2 was assigned, reflecting high uncertainty. <sup>dd</sup>Based on variability in results from Lipscomb et al. (1998b) and Elfarra et al. (1998) in microsomes. Since only pooled or mean values are available, CU of one was assigned (moderate uncertainty). <sup>ee</sup>No data on variability, so a CV of 0.5 was assigned, with a CU of 2. <sup>ff</sup>No data on variability, so a CV of 2 was assigned (larger than assumed for metabolism due to possible vehicle effects), with a CU of 2.

**Table S5.** Interstrain variability parameters.

Interstrain scaling parameter	Parameter scaling	Population mean: Distribution	Population mean: SD or Min	Population mean: Truncation ( $\pm$ nxSD) or Max	Population variance: CV	Population variance: CU
lnISOx	$VMAX \rightarrow VMAX \times \exp(\lnISOx)$	Uniform	-4.605	4.605	2	2
lnISTCA	$\lnFracTCAC \rightarrow \lnFracTCAC + \lnISTCA$	Uniform	-4.605	4.605	2	2
lnISDCA	$FracOther \rightarrow FracOther \times \exp(\lnISDCA)$	Uniform	-4.605	4.605	2	2
lnISConj	$VMAXDCVG \rightarrow VMAXDCVG \times \exp(\lnISConj)$	Uniform	-4.605	4.605	2	2
lnISkTCA	$kUrnTCA \rightarrow kUrnTCA \times \exp(\lnISTCA)$ $kMetTCA \rightarrow kMetTCA \times \exp(\lnISTCA)$	Uniform	-4.605	4.605	2	2
lnISkDCVG	$kDCVG \rightarrow kDCVG \times \exp(\lnISDCVG)$	Uniform	-4.605	4.605	2	2
lnISkDCVC	$kElimDCVC \rightarrow kElimDCVC \times \exp(\lnISDCVG)$	Uniform	-4.605	4.605	2	2

**Table S6.** Comparison of prior and posterior distributions for scaling parameters.

Parameter	Population Mean: Prior Median	Population Mean: Prior 2.5%	Population Mean: Prior 97.5%	Population Mean: Posterior Median	Population Mean: Posterior 2.5%	Population Mean: Posterior 97.5%	Population Variability: Prior CV	Population Variability: Prior CU	Population Variability: Posterior CV	Population Variability: Posterior CU
lnQCC	0	-0.392	0.392	0.152	-0.0798	0.358	0.2	2	0.206	0.214
lnVPRC	0	-0.392	0.392	-0.319	-0.574	-0.0191	0.2	2	0.27	0.301
lnDRespC	-4.61	-11.2	1.96	0.83	0.442	1.3	0.2	0.5	0.212	0.117
lnPRBCPlasTCAC	0	-4.37	4.37	0.889	-0.212	1.74	0.336	2	0.423	0.59
lnkDissocC	0	-2.33	2.33	0.467	-0.713	1.78	1.19	2	1.15	1.18
lnBMaxkDC	0	-0.97	0.97	0.421	-0.0813	0.929	0.495	2	0.45	0.534
lnPeffDCVG	0	-6.56	6.56	0.0903	-5.22	2.46	0.4	2	0.406	0.456
lnPeffDCVC	0	-6.56	6.56	5.98	4.61	6.85	0.4	2	0.408	0.435
lnPeffDCA	0	-6.56	6.56	3.67	-0.355	6.35	0.4	2	0.424	0.473
lnVMaxC	0	-1.36	1.36	-0.633	-1.23	0.00521	0.824	1	0.74	0.568
lnKMC	0	-2.72	2.72	-2.44	-3.41	-1.43	0.27	1	1.01	0.869
lnFracOtherC	0	-6.56	6.56	-4.16	-6.16	-1.95	0.5	2	0.537	0.621
lnFracTCAC	0	-2.28	2.28	-1.43	-2.08	-0.761	0.5	2	0.477	0.573
lnVMaxDCVGC	0	-6.56	6.56	-4.96	-6.46	-3.29	0.5	2	0.525	0.728
lnClDCVGC	0	-6.56	6.56	-3.63	-5.26	1.09	0.5	2	0.551	1.29
lnVMaxLungLivC	0	-2.15	2.15	2.28	0.525	3.11	0.5	2	0.81	1.33
lnKMClara	0	-6.56	6.56	-5.05	-6.56	-3.33	0.5	2	0.571	0.808
lnFracLungSysC	0	-6.56	6.56	2.72	-0.0928	5.41	0.5	2	0.615	1.23
lnVMaxTCOHC	0	-8.75	8.75	1.14	0.477	1.89	0.5	2	0.655	0.455
lnKMTCOH	0	-8.75	8.75	-0.0643	-1.29	0.952	0.5	2	0.554	0.713
lnVMaxGlucC	0	-8.75	8.75	4.63	3.76	6.32	0.5	2	0.501	0.508
lnKMGluc	0	-6.56	6.56	3.41	2.03	5.21	0.5	2	0.606	0.95

Parameter	Population Mean: Prior Median	Population Mean: Prior 2.5%	Population Mean: Prior 97.5%	Population Mean: Posterior Median	Population Mean: Posterior 2.5%	Population Mean: Posterior 97.5%	Population Variability: Prior CV	Population Variability: Prior CU	Population Variability: Posterior CV	Population Variability: Posterior CU
InkMetTCOHC	-2.3	-11.1	6.45	1.98	0.455	3.14	0.5	2	0.591	0.844
InkUrnTCAC	0	-4.37	4.37	-2.11	-3.16	-1.27	0.5	2	0.69	0.635
InkMetTCAC	-2.3	-8.86	4.26	-0.698	-1.34	0.0157	0.5	2	0.474	0.373
InkBileC	-2.3	-8.86	4.26	0.863	-0.192	1.73	0.5	2	0.516	0.611
InkEHRC	-2.3	-8.86	4.26	-3.25	-4.72	-2.39	0.5	2	0.565	0.554
InkUrnTCOGC	0	-6.56	6.56	2.33	0.933	4.39	0.5	2	1.5	1.51
InkDCVGC	-2.3	-8.86	4.26	2.19	0.061	4.4	0.5	2	0.535	0.75
InkElimDCVCC	-2.3	-8.86	4.26	-1.14	-2.3	-0.0474	0.5	2	0.53	0.659
InkClearDCAC	-2.3	-8.86	4.26	-2.57	-8.02	1.34	0.5	2	0.607	1.19
InkDCAcen_perC	-2.3	-8.86	4.26	1.25	-5.28	4.28	0.5	2	0.618	1.12
InkDCAper_cenC	-2.3	-8.86	4.26	-2.14	-5.73	1.72	0.5	2	0.66	0.98
InkTSD	0.336	-4.04	4.71	1.36	-1.02	4.1	2	2	2.12	5.2
InkAS	0.336	-6.23	6.9	-0.0762	-2.04	1.92	2	2	1.69	1.5
InkAD	-0.288	-6.85	6.27	-1.34	-2.74	0.193	2	2	1.52	1.6
InkASTCA	-0.288	-6.85	6.27	1.71	-2.24	5.55	2	2	2.05	2.3
InkASTCOH	-0.288	-6.85	6.27	-0.361	-5.25	4.8	2	2	1.98	2.35
InISOx	0	-4.37	4.37	-0.0614	-1.78	1.96	2	2	1.2	0.767
InISTCA	0	-4.37	4.37	-1.83	-4.23	0.265	2	2	1.53	1.19
InISDCA	0	-4.37	4.37	-0.649	-2.98	1.43	2	2	1.1	0.532
InISConj	0	-4.37	4.37	-1.11	-3.29	0.723	2	2	1.58	1.36
InISkTCA	0	-4.37	4.37	-0.19	-1.4	0.802	2	2	0.96	0.403
InISkDCVG	0	-4.37	4.37	1.24	-0.709	3.37	2	2	1.64	1.15
InISkDCVC	0	-4.37	4.37	-0.654	-2.18	1.22	2	2	1.53	1.09

## Methods

### Details of the Bayesian PBPK modeling of TCE and its metabolites

The structure of the updated PBPK model and the statistical population model are shown graphically in Figure 2 in the manuscript. Details as to the model structure and equations, and the likelihood function used in the parameter estimation, are given below.

#### **PBPK model structure and equations**

The equations below, along with the parameters defined in Supplemental Table S3, specify the PBPK model. The ordinary differential equations are shown in bold, with the remaining equations being algebraic definitions. The same equations are in the PBPK model code, with some additional provisions for unit conversions (e.g., ppm to mg/L) or numerical stability (e.g., truncating small values at  $10^{-15}$ , so states are never negative). For reference, the stoichiometric adjustments for molecular weights are given by the following:

#### # Molecular Weights

TCE:            MW<sub>TCE</sub> = 131.39

DCA:            MW<sub>DCA</sub> = 129.0

DCVC:          MW<sub>DCVC</sub> = 216.1

TCA:            MW<sub>TCA</sub> = 163.5

TCOH:          MW<sub>TCOH</sub> = 149.5

TCOG:          MW<sub>TCOHGluC</sub> = 325.53

#### # Stoichiometry

StochTCATCE = MW<sub>TCA</sub>/MW<sub>TCE</sub>;

StochTCATCOH = MW<sub>TCA</sub>/MW<sub>TCOH</sub>;

StochTCOHTCE = MW<sub>TCOH</sub>/MW<sub>TCE</sub>;

StochGlucTCOH = MWTCOHHGluc/MWTCOH;

StochTCOHHGluc = MWTCOH/MWTCOHHGluc;

StochTCEGluc = MWTCE/MWTCOHHGluc;

StochDCVCTCE = MWDCVC/MWTCE

### **TCE submodel**

The TCE submodel is a whole-body, flow-limited PBPK model, with gas respiratory exchange, oral absorption, and metabolizing and nonmetabolizing tissues.

#### ***Gas exchange, respiratory metabolism, arterial blood concentration, and closed-chamber concentrations***

For an open-chamber concentration and a closed-chamber concentration of ACh/VCh, the rates of change for the amount in the respiratory lumen during inhalation (AIinhResp, in mg), the amount in the respiratory tract tissue (Aresp, in mg), and the respiratory lumen during exhalation (AExhResp, in mg) are given by the following:

$$\frac{d(AInhResp)}{dt} = (QM \times CInh + DResp \times (CResp - CInhResp) - QM \times CInhResp) \quad [Eq. 1]$$

$$\frac{d(Aresp)}{dt} = (DResp \times (CInhResp + CExhResp - 2 \times CResp) - RAMetLng) \quad [Eq. 1]$$

$$\frac{d(AExhResp)}{dt} = (QM \times (CInhResp - CExhResp) + QP \times (CArt\_tmp/PB-CInhResp) + DResp \times (CResp-CExhResp)) \quad [Eq. 2]$$

where

CInh = inhaled concentration (mg/L) = ACh/VCh + Conc

QM = minute volume (L/hour) = QP/0.7

CInhResp = concentration in respiratory lumen during inhalation (mg/L)  
= AIinhResp/VRespLum

CResp = concentration in respiratory tract tissue (mg/L)  
= Aresp/VRespEff

CExhResp	= concentration in respiratory lumen during exhalation (mg/L) = AExhResp/VRespLum
RAMetLng	= rate of metabolism in respiratory tract tissue = (VMAXClara × CResp)/(KMC Clara + CResp)
CArt_tmp	= arterial blood concentration after gas exchange = (QC × CVen + QP × CIinhResp)/(QC + (QP/PB))

Because alveolar breath concentrations can include desorption from the respiratory tract tissue, the concentration at the alveolae (CArt\_tmp/PB) may not equal the measured concentration in end-exhaled breath. It is therefore assumed that the ratio of the measured end-exhaled breath concentration to the concentration in the absence of desorption is the same as the ratio of the rate of TCE leaving the lumen to the rate of TCE entering the lumen:

$$CAlv/(CArt\_tmp/PB) = (QM \times CMixExh)/\{(QP \times CArt\_tmp/PB) + (QM-QP) \times CIinhResp\} \quad [Eq. 3]$$

That is, it is assumed that desorption occurs proportionally throughout the “breath.” The concentration of arterial blood entering circulation needs to add the contribution from the i.a. dose (IADose in mg/kg, infused over a time period TChng):

$$CArt = CArt\_tmp + kIA/QC \quad [Eq. 4]$$

where

$$kIA = (IADose \times \text{body weight})/TChng$$

For closed-chamber experiments, the additional differential equation for the amount in the chamber (ACh, in mg) is:

$$d(ACh)/dt = Rodents \times (QM \times CMixExh - QM \times ACh/VCh) - kLoss \times Ach \quad [Eq. 5]$$

where rodents is the number of animals in the chamber, and kLoss is the chamber loss rate (per hour).

### ***Oral absorption to gut compartment***

For oil-based gavage, the dose PDose is defined in terms of units of mg/kg, entering the stomach during a time TChng, with rates of change in the stomach (AStom, in mg) and duodenum (ADuod, in mg):

$$d(AStom)/dt = kStom - AStom \times (kAS + kTSD) \quad [\text{Eq. 6}]$$

$$d(ADuod)/dt = (kTSD \times AStom) - kAD \times ADuod \quad [\text{Eq. 7}]$$

where

$$kStom = \text{rate of TCE entering stomach (mg/hour)} = (PDose \times \text{body weight})/TChng$$

Note that there is absorption to the gut from both the stomach and duodenal compartments. Analogous equations are defined for aqueous gavage, with the expectation that absorption and transfer coefficients would differ with the different vehicle. In particular, the aqueous gavage dose PDoseAq is defined in terms of units of mg/kg, entering the stomach during a time TChng, with rates of change in the stomach (AStomAq, in mg) and duodenum (ADuodAq, in mg):

$$d(AStomAq)/dt = kStomAq - AStomAq \times (kASAq + kTSDAq) \quad [\text{Eq. 8}]$$

$$d(ADuodAq)/dt = (kTSDAq \times AStomAq) - kADAq \times ADuodAq \quad [\text{Eq. 9}]$$

where

$$kStomAq = \text{rate of TCE entering stomach (mg/hour)} = (PDoseAq \times \text{body weight})/TChng$$

For drinking water, the rate Drink is defined in terms of mg/kg-day, and it is assumed that absorption is direct to the gut:

$$kDrink = (\text{Drink} \times \text{body weight})/24.0 \quad [\text{Eq. 10}]$$

Therefore, the total rate of absorption to the gut via oral exposure (RAO, in mg/hour) is:

$$\begin{aligned} RAO &= kDrink + (kAS \times AStom) + (kAD \times ADuod) + (kASAq \\ &\quad \times AStomAq) + (kADAq \times ADuodAq) \end{aligned} \quad [\text{Eq. 11}]$$

The differential equation for the gut compartment (AGut, in mg) is, therefore, given by:

$$d(AGut)/dt = QGut \times (CArt - CVGut) + RAO \quad [Eq. 12]$$

where

$$CVGut = \text{concentration in the gut (mg/L)} = AGut/VGut/PGut$$

### ***Nonmetabolizing tissues***

The differential equations for nonmetabolizing tissues (rapidly perfused, ARap, in mg; slowly perfused, ASlw, in mg; fat, AFat, in mg; and kidney, AKid, in mg) follow the standard flow-limited form:

$$d(ARap)/dt = QRap \times (CArt - CVRap) \quad [Eq. 13]$$

$$d(ASlw)/dt = QSlw \times (CArt - CVSlw) \quad [Eq. 14]$$

$$d(AFat)/dt = QFat \times (CArt - CVFat) \quad [Eq. 15]$$

$$d(AKid)/dt = (QKid \times (CArt - CVKid)) \quad [Eq. 16]$$

where

$$\begin{aligned} CVRap &= \text{venous blood concentration leaving rapidly perfused issues} \\ &= ARap/VRap/PRap \end{aligned}$$

$$\begin{aligned} CVSlw &= \text{venous blood concentration leaving slowly perfused issues} \\ &= ASlw/VSlw/PSlw \end{aligned}$$

$$\begin{aligned} CVFat &= \text{venous blood concentration leaving fat} \\ &= AFat/VFat/PFat \end{aligned}$$

$$\begin{aligned} CVKid &= \text{venous blood concentration leaving kidney} \\ &= AKid/VKid/PKid \end{aligned}$$

Chiu et al. (2009) and Evans et al. (2009) included kidney GSH conjugation. For the current effort, it was determined to be non-identifiable as compared to liver GSH conjugation.

### ***Liver compartment***

The liver has two metabolizing pathways:

$$\begin{aligned} \text{RAMetLiv1} &= \text{Rate of TCE oxidation by P450 in liver (mg/hour)} \\ &= (\text{VMAX} \times \text{CVLiv}) / (\text{KM} + \text{CVLiv}) \end{aligned} \quad [\text{Eq. 17}]$$

$$\begin{aligned} \text{RAMetLiv2} &= \text{Rate of TCE metabolized to S-dichlorovinyl glutathione (DCVG) in liver (mg/hour)} \\ &= (\text{VMAXDCVG} \times \text{CVLiv}) / (\text{KMDCVG} + \text{CVLiv}) \end{aligned} \quad [\text{Eq. 18}]$$

Some experiments also had portal vein dosing (PVDOSE in mg/kg, infused over a time period TChng), with a rate entering the liver of:

$$kPV = (PVDOSE \times \text{body weight}) / TChng \quad [\text{Eq. 19}]$$

The differential equation for TCE in liver (ALiv, in mg) is thus:

$$d(ALiv)/dt = (QLiv \times (CArt - CVLiv)) + (QGut \times (CVGut - CVLiv)) - RAMetLiv1 - RAMetLiv2 + kPV \quad [\text{Eq. 20}]$$

where

$$\begin{aligned} \text{CVLiv} &= \text{venous blood concentration leaving liver} \\ &= ALiv/VLiv/PLiv \end{aligned}$$

### ***Venous blood compartment***

The venous blood compartment (ABld, in mg) has inputs both from the venous blood exiting tissues as well as from an IV dose (IVDose in mg/kg infused during a time TChng), and output to the gas exchange region:

$$\begin{aligned} d(ABld)/dt &= (QFat \times CVFat + QGutLiv \times CVLiv + QSlw \\ &\quad \times CVSlw + QRap \times CVRap + QKid \times CVKid) \\ &\quad + kIV - CVen \times QC \end{aligned} \quad [\text{Eq. 21}]$$

where

$$\begin{aligned} kIV &= \text{IV infusion rate} \\ &= (IVDose \times \text{body weight}) / TChng \end{aligned}$$

$$\begin{aligned} CVen &= \text{concentration in mixed venous blood} \\ &= ABld/VBld \end{aligned}$$

### ***TCOH Submodel***

The TCOH submodel is a simplified whole-body, flow-limited PBPK model, with only a body (ABodTCOH, in mg) and liver (ALivTCOH, in mg) compartment.

#### ***Blood concentration***

The venous blood concentration, including an IV dose (IVDoseTCOH in mg/kg infused during a time TChng), is given by

$$CTCOH = (QBod \times CVBodTCOH + QGutLiv \times CVLivTCOH + kIVTCOH)/QC \quad [\text{Eq. 22}]$$

where

$$CVBodTCOH = ABodTCOH/VBodTCOH/PBodTCOH$$

$$CVLivTCOH = ALivTCOH/VLiv/PLivTCOH$$

$$\begin{aligned} kIVTCOH &= \text{IV infusion rate} \\ &= (\text{IVDoseTCOH} \times \text{body weight})/\text{TChng} \end{aligned}$$

and the partition coefficients for the body:blood and liver:blood are PBodTCOH and PLivTCOH, respectively, QGutLiv is the sum of the portal vein and hepatic artery blood flows, QBod is the remaining blood flow, VLiv is the liver volume, and VBodTCOH is the remaining perfused volume.

#### ***Body compartment***

The rate of change of the amount of TCOH in the body compartment is

$$d(ABodTCOH)/dt = QBod \times (CTCOH - CVBodTCOH) \quad [\text{Eq. 23}]$$

### **Liver compartment**

The liver has three metabolizing pathways:

$$\begin{aligned} \text{RAMetTCOHTCA} &= \text{Rate of oxidation of TCOH to TCA (mg/hour)} & [\text{Eq. 24}] \\ &= (\text{VMAXTCOH} \times \text{CVLivTCOH}) / (\text{KMTCOH} \\ &\quad + \text{CVLivTCOH}) \end{aligned}$$

$$\begin{aligned} \text{RAMetTCOHHGluc} &= \text{Amount of glucuronidation to TCOG (mg/hour)} & [\text{Eq. 25}] \\ &= (\text{VMAXGluc} \times \text{CVLivTCOH}) / (\text{KMGluc} \\ &\quad + \text{CVLivTCOH}) \end{aligned}$$

$$\begin{aligned} \text{RAMetTCOH} &= \text{Amount of TCOH metabolized to other (e.g., DCA)} & [\text{Eq. 26}] \\ &= k_{\text{MetTCOH}} \times A_{\text{LivTCOH}} \end{aligned}$$

Some experiments also had oral dosing (PODoseTCOH in mg/kg, entering the stomach over a time TChng):

$$d(A_{\text{StomTCOH}})/dt = k_{\text{StomTCOH}} - A_{\text{StomTCOH}} \times k_{\text{ASTCOH}} & [\text{Eq. 27}]$$

$$k_{\text{StomTCOH}} = (\text{PODoseTCOH} \times \text{body weight}) / \text{TChng} & [\text{Eq. 28}]$$

$$k_{\text{POTCOH}} = A_{\text{StomTCOH}} \times k_{\text{ASTCOH}} & [\text{Eq. 29}]$$

In addition, there are three additional sources of TCOH:

$$\begin{aligned} \text{Production in the liver from TCE (a fraction of hepatic oxidation)} & & [\text{Eq. 30}] \\ &= (1.0 - \text{FracOther} - \text{FracTCA}) \times \text{StochTCOHTCE} \times \text{RAMetLiv1} \end{aligned}$$

$$\begin{aligned} \text{Production in the lung from TCE (a fraction of lung oxidation)} & & [\text{Eq. 31}] \\ &= (1.0 - \text{FracOther} - \text{FracTCA}) \times \text{StochTCOHTCE} \\ &\quad \times \text{FracLungSys} \times \text{RAMetLng} \end{aligned}$$

$$\begin{aligned} \text{Enterohepatic recirculation (rate kEHR) from TCOG in the bile} & & [\text{Eq. 32}] \\ (\text{amount ABileTCOG}) &= \text{StochTCOHHGluc} \times \text{RARecircTCOG} \\ &= \text{StochTCOHHGluc} \times k_{\text{EHR}} \times \text{ABileTCOG} \end{aligned}$$

Note that StochTCOHTCE is the ratio of molecular weights of TCOH and TCE, StochTCOHHGluc is the ratio of molecular weights of TCOH and TCOG, FracOther is the fraction of TCE oxidation not producing TCA or TCOH, FracTCA is the fraction of TCE

oxidation producing TCA, and FracLungSys is the fraction of lung TCE oxidation that is translocated to the liver and not locally cleared.

The differential equation for TCOH in liver (ALivTCOH, in mg) is thus:

$$\begin{aligned} d(ALivTCOH)/dt = & kPOTCOH + QGutLiv \times (CTCOH - CVLivTCOH) & [Eq. 33] \\ & - RAMetTCOH - RAMetTCOHTCA - RAMetTCOHTCOH \\ & + ((1.0 - FracOther - FracTCA) \times StochTCOHTCE \\ & \times (RAMetLiv1 + FracLungSys \times RAMetLng)) \\ & + (StochTCOHTCOH \times RARecircTCOG) \end{aligned}$$

### ***TCOG Submodel***

The TCOG submodel is a simplified whole-body, flow-limited PBPK model, with body (ABodTCOG, in mg), liver (ALivTCOG, in mg), and bile (ABileTCOG) compartments.

### ***Blood concentration***

The venous blood concentration is given by:

$$CTCOG = (QBod \times CVBodTCOG + QGutLiv \times CVLivTCOG)/QC \quad [Eq. 34]$$

where

$$CVBodTCOG = ABodTCOG/VBodTCOH/PBodTCOG$$

$$CVLivTCOG = ALivTCOG/VLiv/PLivTCOG$$

and the partition coefficients for the body:blood and liver:blood are PBodTCOG and PLivTCOG, respectively, QGutLiv is the sum of the portal vein and hepatic artery blood flows, QBod is the remaining blood flow, VLiv is the liver volume, and VBodTCOH is the remaining perfused volume.

### ***Body compartment***

The body compartment is flow limited, with urinary excretion rate (mg/hour):

$$RUrnTCOG = kUrnTCOG \times ABodTCOG \quad [\text{Eq. 35}]$$

So the rate of change of the amount of TCOG in the body compartment is:

$$d(ABodTCOG)/dt = QBod \times (CTCOG - CVBodTCOG) - RUrnTCOG \quad [\text{Eq. 36}]$$

Thus, the amount excreted in urine ( $AUrnTCOG$ , mg) is given by:

$$d(AUrnTCOG)/dt = RUrnTCOG \quad [\text{Eq. 37}]$$

### ***Liver compartment***

The liver is flow limited, with one input, glucuronidation of TCOH (defined above in the TCOH submodel):

$$\text{StochGlucTCOH} \times \text{RAMetTCOHHGluc} \quad [\text{Eq. 38}]$$

and one additional output, excretion in bile:

$$RBileTCOG = \text{rate of excretion in bile (mg/hour)} = kBile \times ALivTCOG \quad [\text{Eq. 39}]$$

The rate of change of the amount of TCOG in the liver is, therefore:

$$\begin{aligned} d(ALivTCOG)/dt &= QGutLiv \times (CTCOG - CVLivTCOG) \\ &\quad + (\text{StochGlucTCOH} \times \text{RAMetTCOHHGluc}) - RBileTCOG \end{aligned} \quad [\text{Eq. 40}]$$

### ***Bile compartment***

The bile compartment has one input, excretion of TCOG in bile from the liver (defined above) and one output, enterohepatic recirculation to TCOH in the liver (defined above in the TCOH submodel), with rate of change:

$$d(ABileTCOG)/dt = RBileTCOG - RARecircTCOG \quad [\text{Eq. 41}]$$

### **TCA Submodel**

The TCA submodel is the same as that in Hack et al. (2006), with an error in the plasma flow to the liver corrected. In brief, TCA in plasma is assumed to undergo saturable plasma protein binding. TCA in tissues is assumed to be flow limited, but with the tissue partition coefficient reflecting equilibrium with the free concentration of TCA in plasma.

### **Plasma binding and concentrations**

For an i.v. dose of TCA given by  $\text{IVDoseTCA}$  (mg/kg during an infusion period of  $\text{TChng}$ ), the rate of the change of the amount of total TCA in plasma ( $\text{APlasTCA}$ , in mg) is:

$$\frac{d(\text{APlasTCA})}{dt} = \text{kIVTCA} + (\text{QBodPlas} \times \text{CVBodTCA}) + (\text{QGutLivPlas} \times \text{CVLivTCA}) - (\text{QCPlas} \times \text{CPlasTCA}) - \text{RUrnTCApas} \quad [\text{Eq. 42}]$$

where

$\text{kIVTCA}$  = rate of IV infusion of TCA =  $(\text{IVDoseTCA} \times \text{body weight})/\text{TChng}$

$\text{QBodPlas}$  = plasma flow from body =  $\text{QBod} \times \text{FracPlas}$

$\text{QGutLivPlas}$  = plasma flow from liver =  $(\text{QGut} + \text{QLiv}) \times \text{FracPlas}$

$\text{CVBodTCA}$  = venous concentration leaving body =  $\text{CPlasTCABnd} + \text{CVBodTCAPFree}$

$\text{CVBodTCAPFree}$  = free venous concentration leaving body  
=  $(\text{ABodTCA}/\text{VBod}/\text{PBodTCA})$

$\text{CVLivTCA}$  = venous concentration leaving liver  
=  $\text{CPlasTCABnd} + \text{CVLivTCAPFree}$

$\text{CVLivTCAPFree}$  = free venous concentration leaving liver  
=  $(\text{ALivTCA}/\text{VLiv}/\text{PLivTCA})$

$\text{QCPlas}$  = total plasma flow  
=  $\text{QC} \times \text{FracPlas}$

$\text{RUrnTCApas}$  = rate of urinary excretion of TCA from plasma  
=  $\text{kUrnTCA} \times \text{APlasTCAPFree}$

The free ( $C_{PlasTCAFree}$ ) and bound ( $C_{PlasTCABnd}$ ) concentrations are calculated from the total concentration ( $C_{PlasTCA} = A_{PlasTCA}/V_{Plas}$ ) by solving the equations:

$$C_{PlasTCABndMole} = B_{Max} \times C_{PlasTCAFreeMole}/(k_{Dissoc} + C_{PlasTCAFreeMole}) \quad [Eq. 43]$$

$$C_{PlasTCABndMole} = C_{PlasTCAMole} - C_{PlasTCAFreeMole} \quad [Eq. 44]$$

Here the suffix “Mole” means that all concentrations are in micromole/L, because  $B_{Max}$  and  $k_{Dissoc}$  are given in those units. These lead to explicit solutions of:

$$C_{PlasTCAFreeMole} = (sqrt(a \times a + b) - a)/2 \quad [Eq. 45]$$

where

$$a = k_{Dissoc} + B_{Max} - C_{PlasTCAMole}$$

$$b = 4.0 \times k_{Dissoc} \times C_{PlasTCAMole}$$

$$C_{PlasTCABnd} = C_{PlasTCAMole} - C_{PlasTCAFree}$$

These concentrations are converted to mg/L ( $C_{PlasTCABnd}$ ,  $C_{PlasTCAFree}$ ) by multiplying by the molecular weight in mg/ $\mu$ moles. The amount of free TCA in plasma is, thus:

$$A_{PlasTCAFree} = C_{PlasTCAFree} \times V_{Plas}. \quad [Eq. 46]$$

Here,  $V_{Plas}$  is derived from the blood volume and hematocrit.

### ***Urinary excretion***

Urinary excretion is modeled as coming from the plasma compartment, so the rate of change of TCA in urine ( $A_{UrnTCA}$ , in mg) is:

$$d(A_{UrnTCA})/dt = R_{UrnTCA} \quad [Eq. 47]$$

where

$$R_{UrnTCA} = R_{UrnTCAPlas}$$

For some human data (Chiu et al. 2007), urinary excretion was only collected during certain time periods, with data missing in other time periods. Thus, a switch UrnMissing was defined, which equals 0 during times of urine collection and 1 when urinary data are missing (this parameter was not used for mice, and set to 0). The total amount of urinary TCA “collected” (AUrnTCA\_collect, in mg) is, thus, given by:

$$d(AUrnTCA_{collect})/dt = (1-UrnMissing) \times RUrnTCA \quad [Eq. 48]$$

### ***Body compartment***

The body compartment is flow limited, with the rate of change for the amount of TCA in the body (ABodTCA, in mg) given by:

$$d(ABodTCA)/dt = QBodPlas \times (CPlasTCAF - CVBodTCAF) \quad [Eq. 49]$$

### ***Liver compartment***

The rate of change for the amount of TCA in the liver (ALivTCA, in mg) is given by:

$$\begin{aligned} d(ALivTCA)/dt = & QGutLivPlas \times (CPlasTCAF - CVLivTCAF) \quad [Eq. 50] \\ & + (\text{FracTCA} \times \text{StochTCATCE} \times (\text{RAMetLiv1} + \text{FracLungSys} \times \text{RAMetLng})) \\ & + (\text{StochTCATCOH} \times \text{RAMetTCOHTCA}) - \text{RAMetTCA} + kPOTCA \end{aligned}$$

The first term reflects the free TCA in plasma flowing into and out of the liver compartment, the second term reflects production of TCA from liver (adjusted for molecular weights and fractional yield of TCA) and lung (adjusted for molecular weights, fraction of lung metabolism translocated to the liver, and fractional yield of TCA) metabolism of TCE, the third term reflects production of TCA from TCOH, the fourth term reflects other clearance of TCA from the liver, and the fifth term reflects absorption from the stomach of TCA. The contribution from liver metabolism of TCE is adjusted for molecular weights and production of oxidative metabolites other than TCA. The rate of clearance of TCA is given by:

$$RAMetTCA = kMetTCA \times ALivTCA \quad [Eq. 51]$$

The oral intake rate of TCA (mg/hour) includes a one-compartment stomach. So for an oral dose of PODoseTCA (in mg/kg), occurring over a time TChng, the rate of change of TCA in the stomach (ASTomTCA, in mg) is given by:

$$d(AStomTCA)/dt = kStomTCA - AStomTCA \times kASTCA \quad [Eq. 52]$$

where

$$\begin{aligned} kStomTCA &= \text{rate of input into stomach} \\ &= (PODoseTCA \times \text{body weight})/TChng \end{aligned}$$

The rate of absorption into the liver is, thus,

$$kPOTCA = AStomTCA \times kASTCA \quad [Eq. 53]$$

### ***GSH conjugation submodel***

The GSH conjugation submodel only tracks DCVG, DCVC, and elimination of DCVC.

The rate of change for DCVG (ADCVGmol, in mmoles) depends on production from TCE in the liver and metabolism to DCVC:

$$d(ADCVGmol)/dt = RAMetLiv2/MWTCE - RAMetDCVGmol \quad [Eq. 54]$$

where

$$\begin{aligned} RAMetDCVGmol &= \text{rate of metabolism of DCVG to DCVC} \\ &= kDCVG \times ADCVGmol \end{aligned}$$

The rate of change of DCVC (ADCVC, in mg) depends on the production from DCVG and the lumped elimination rate of DCVC (rate constant kElimDCVC):

$$d(ADCVC)/dt = RAMetDCVGmol \times MWDCVC - kElimDCVC \times ADCVC \quad [Eq. 55]$$

### ***DCA submodel***

The DCA submodel is a two-compartment model with a central and peripheral compartment, with clearance (lumped metabolism and excretion) from the central compartment.

The rate of change for DCA in the central compartment (ADCA, in mg) depends on the production from TCE metabolism, the clearance (rate constant kClearDCA), and distribution to (rate constant kDCAcen\_per) and from (rate constant kDCAper\_cen) the peripheral compartment:

$$\begin{aligned} \frac{d(ADCA)}{dt} = & (FracOther \times StochDCATCE \times (RAMetLiv1 \\ & + FracLungSys \times RAMetLng)) - (kClearDCA \times ADCA) - kDCAcen\_per \times \\ & ADCA \\ & + kDCAper\_cen \times ADCaper; \end{aligned} \quad [\text{Eq. 56}]$$

The rate of change for DCA in the peripheral compartment (ADCaper, in mg) depends only on the distribution to and from the central compartment:

$$\frac{d(ADCaper)}{dt} = kDCAcen\_per \times ADCA - kDCAper\_cen \times ADCaper \quad [\text{Eq. 57}]$$

### *Likelihood function*

In most cases, the likelihood function of the data given the predictions was assumed to be lognormal, which requires specification of the variance of the “residual error.” This error may include variability due to measurement error, intra-individual and intra-study heterogeneity, as well as model misspecification. The variances for each of the corresponding residual errors were given log-uniform distributions. For all measurements, the bounds on the log-uniform distribution were 0.01 and 3.3, corresponding to geometric standard deviations bounded by 1.11 and 6.15. The lower bound was set to prevent “over-fitting” (Bois 2000; CE Hack et al. 2006). The upper bound was set at an arbitrarily high value, and the posteriors checked to make sure that the bound was unimportant.

For DCVG, DCVC, and DCA data, a different error model was necessary because many individual measurements were below the limit of quantitation. The use of a lognormal error model is based on the fact that analytical measurements typically have proportional errors well

above the detection limit. However, much of the data on DCVG, DCVC, and DCA are at or near the detection limit, where analytical errors are typically fixed and a normal distribution is more appropriate. Therefore, for these data, a “two-component error model” (Rocke and Lorenzato 1995) was used that is normally distributed near the detection limit (with a standard deviation fixed at one-third of the detection limit) and lognormally distributed well above the detection limit (with “residual error” specified as discussed previously). Specifically, the variance-stabilizing “generalized-log” transformation (Durbin and Rocke 2003) was employed for computing the likelihood.

## References

- Abbas R, Fisher J. 1997. A physiologically based pharmacokinetic model for trichloroethylene and its metabolites, chloral hydrate, trichloroacetate, dichloroacetate, trichloroethanol, and trichloroethanol glucuronide in B6C3F1 mice. *Toxicol Appl Pharmacol* 147(1):15-30.
- Barter Z, Bayliss M, Beaune P, Boobis A, Carlile D, Edwards R, et al. 2007. Scaling factors for the extrapolation of in vivo metabolic drug clearance from in vitro data: Reaching a consensus on values of human microsomal protein and hepatocellularity per gram of liver. *Curr Drug Metab* 8(1):33-45.
- Bronley-DeLancey A, McMillan D, McMillan J, Jollow D, Mohr L, Hoel D. 2006. Application of cryopreserved human hepatocytes in trichloroethylene risk assessment: Relative disposition of chloral hydrate to trichloroacetate and trichloroethanol. *Environ Health Perspect* 114(8):1237-1242.
- Brown R, Delp M, Lindstedt S, Rhomberg L, Beliles R. 1997. Physiological parameter values for physiologically based pharmacokinetic models. *Toxicol Ind Health* 13(4):407-484.
- Evans MV, Chiu WA, Okino MS, Caldwell JC. 2009. Development of an updated PBPK model for trichloroethylene and metabolites in mice, and its application to discern the role of oxidative metabolism in TCE-induced hepatomegaly. *Toxicol Appl Pharmacol* 236(3):329-340.
- Elfarra A, Krause R, Last A, Lash L, Parker J. 1998. Species- and sex-related differences in metabolism of trichloroethylene to yield chloral and trichloroethanol in mouse, rat, and human liver microsomes. *Drug Metab Dispos* 26(8):779-785.
- Fisher J, Gargas M, Allen B, Andersen M. 1991. Physiologically based pharmacokinetic modeling with trichloroethylene and its metabolite, trichloroacetic acid, in the rat and mouse. *Toxicol Appl Pharmacol* 109(2):183-195.
- Green T, Mainwaring G, Foster J. 1997. Trichloroethylene-induced mouse lung tumors: Studies of the mode of action and comparisons between species. *Fundam Appl Toxicol* 37(2):125-130.
- Hejtmancik M, Trela B, Kurtz P, Persing R, Ryan M, Yarrington J, et al. 2002. Comparative gavage subchronic toxicity studies of o-chloroaniline and m-chloroaniline in F344 rats and B6C3F1 mice. *Toxicol Sci* 69(1):234-243.

- ICRP. 2003. Basic anatomical and physiological data for use in radiological protection: Reference values. (Annals of the ICRP). ICRP Publication 89. New York, NY: Pergamon Press.
- Lash L, Visarius T, Sall J, Qian W, Tokarz J. 1998. Cellular and subcellular heterogeneity of glutathione metabolism and transport in rat kidney cells. *Toxicology* 130(1):1-15.
- Lash L, Xu Y, Elfarra A, Duescher R, Parker J. 1995. Glutathione-dependent metabolism of trichloroethylene in isolated liver and kidney cells of rats and its role in mitochondrial and cellular toxicity. *Drug Metab Dispos* 23(8):846-853.
- Lin Y, Brunt E, Bowling W, Hafenrichter D, Kennedy S, Flye M, et al. 1995. Ras-transduced diethylnitrosamine-treated hepatocytes develop into cancers of mixed phenotype in vivo. *Cancer Res* 55(22):5242-5250.
- Lipscomb J, Fisher J, Confer P, Byczkowski J. 1998a. In vitro to in vivo extrapolation for trichloroethylene metabolism in humans. *Toxicol Appl Pharmacol* 152(2):376-387.
- Lipscomb J, Garrett C, Snawder J. 1997. Cytochrome P450-dependent metabolism of trichloroethylene: Interindividual differences in humans. *Toxicol Appl Pharmacol* 142(2):311-318.
- Lipscomb J, Garrett C, Snawder J. 1998b. Use of kinetic and mechanistic data in species extrapolation of bioactivation: Cytochrome P-450 dependent trichloroethylene metabolism at occupationally relevant concentrations. *J Occup Health* 40(2):110-117.
- Lumpkin M, Bruckner J, Campbell J, Dallas C, White C, Fisher J. 2003. Plasma binding of trichloroacetic acid in mice, rats, and humans under cancer bioassay and environmental exposure conditions. *Drug Metab Dispos* 31(10):1203-1207.
- Sarangapani R, Gentry P, Covington T, Teeguarden J, Clewell HJ I. 2003. Evaluation of the potential impact of age- and gender-specific lung morphology and ventilation rate on the dosimetry of vapors. *Inhal Toxicol* 15(10):987-1016.
- Schultz I, Merdink J, Gonzalez-Leon A, Bull R. 1999. Comparative toxicokinetics of chlorinated and brominated haloacetates in F344 rats. *Toxicol Appl Pharmacol* 158(2):103-114.
- Templin M, Parker J, Bull R. 1993. Relative formation of dichloroacetate and trichloroacetate from trichloroethylene in male B6C3F1 mice. *Toxicol Appl Pharmacol* 123(1):1-8.

Templin M, Stevens D, Stenner R, Bonate P, Tuman D, Bull R. 1995. Factors affecting species differences in the kinetics of metabolites of trichloroethylene. *J Toxicol Environ Health* 44(4):435-447.

Yu K, Barton H, Mahle D, Frazier J. 2000. In vivo kinetics of trichloroacetate in male Fischer 344 rats. *Toxicol Sci* 54(2):302-311.